Int. J. Electrochem. Sci., 16**(2021)** Article ID: 210926, doi: 10.20964/2021.09.37

International Journal of
ELECTROCHEMICAL
SCIENCE
www.electrochemsci.org

Experimental on the Electrokinetic Remediation of Pb(II) Contaminated Loess

Gang Li[1], *Jinli Zhang*[2,*], *Jia Liu*[3], *Shasha Yang*[1], *Shuai Li*[2]

[1] Shaanxi Key Laboratory of Safety and Durability of Concrete Structures, Xijing University, Xi'an, Shaanxi 710123, China;
[2] State Key Laboratory of Coastal and Offshore Engineering, Dalian University of Technology, Dalian, Liaoning 116024, China;
[3] School of Geological Engineering and Geomatics, Chang'an University, Xi'an, Shaanxi 710054, China.
[*]E-mail: jlzhang@dlut.edu.cn

Received: 14 May 2021/ *Accepted:* 5 July 2021 / *Published:* 10 August 2021

Pb(II) accumulates in the human body through the food chain or drinking water and thus causes damage to the nervous, hematological, gastrointestinal, cardiovascular, and renal systems. To effectively suppress the spread of Pb(II) contamination, electrokinetic remediation (ER) tests were conducted on Pb(II)-contaminated loess, and the distribution laws of current (*I*), potential (*U*), pH, Pb(II) concentration (*C*), removal efficiency (*R*), and energy consumption (*E*) during ER process were analyzed. The results revealed that the irregular laws of *I* and *U* over time and a significantly larger range of *I* change in the flow-plastic than in the hard-plastic state. When electrolyte was added to the cathode, the pH value in the soil gradually decreased from the cathode area to the anode area and was distributed between 3 and 6. In the meantime, the Pb(II) *R* reached a maximum of 93.84% and a minimum of 4.29%. The application of ER method resulted in a larger Pb(II) *R* and lower average *E*, suggesting that adding a electrolyte to the cathode, preacidizing treatment, and stirring soil at a fixed interval can significantly improved the remediation efficiency of Pb(II) contaminated loess.

Keywords: Electrokinetic remediation; Pb(II); loess; removal efficiency; energy consumption

1. INTRODUCTION

In recent years, with the continuous acceleration of industrialization and urbanization, the problem of heavy metal-contaminated soil has become increasingly severe. Heavy metal contamination severely affects soil quality and the ecological environment, inhibits vegetation growth, and reduces crop yields. In addition, heavy metals accumulate in the human body through the food chain or drinking water, which causes severe harm to human life and physical health. Lead (Pb)

contamination, a typical representative of the three major types of heavy metal contamination, mainly comes from mining, batteries, dyes, petroleum, and food. When entering the human body, Pb causes adverse effects to the nervous, hematological, gastrointestinal, cardiovascular, and renal systems. Most notably, Pb causes irreversible damage to children's growth and intellectual development. Currently, the main remediation methods of lead-contaminated soil include physical, chemical, biological, and electrokinetic remediation (ER). The basic principle of ER is to insert two electrodes into the soil to form a direct current (DC) electric field between the electrodes. Under the action of the electric field, the charged pollutants in the free state in the soil undergo directional migration (the combined effect of electro migration and electro dialysis). Subsequently, the target pollutants in the cathode and anode areas are treated centrally to accomplish soil remediation. ER is characterized by simple operation, a short remediation cycle, high remediation efficiency, and no environmental contamination. Therefore, this technique has a wide range of application prospects.

Hansen et al. [1] concluded that the ER was effective to removal Cu and Cr from polluted soil, and Cu, Zn and Pb were desorbed at pH values varied from 3 to 4, indicating that the effect of pH on the desorption of heavy metal ions was significant. Beyrami [2] investigated the removal characteristics of Zn, Pb and Cd from calcareous soil using ER, and found that the removal efficiency (*R*) reached 40.11%, 24.70%, and 43.10, respectively. Asadollahfardi et al. [3] studied the removal performance of Pb and Zn from real mine tailing using ER, and revealed that the *R* attained 51.31% and 38.34%, respectively, and increasing the acetic acid concentration was significant improve the removal of both heavy metals. Zulfiqar et al. [4] analyzed the mobility perturbation of Pb(II) by Fe(II) in contaminated soil, and pointed out that Fe(II) improved the adsorption of Pb(II), while Fe(II) with lower ionic conductivity decreased mobility of other particles in contaminated soil. Han et al. [5] noted that the removal of Cd, Cu, Pb, and Zn was remarkable using ER, and *R* improved by EDTA was better than acetic acid. Huang et al. [6] studied the effect of ultrasound-enhanced ER on Zn, Pb, Cu, and Cd removal from fly ashes, and concluded that the acoustic time significantly affected the extraction efficiencies of metal ions in the municipal solid waste. Based on electrical fields and chelating agents method, Tahmasbian and Sinegani [7] indicated that the soluble-exchangeable fraction of Pb and Zn were decreased in the cathodic soil, whereas the carbonate-bound fractions were increased. In the meantime, EDTA enhanced the soluble-exchangeable form of the metals in both anodic and cathodic soils. Zhang et al. [8] revealed that the *R* of Pb increased significantly with the decrease of the pH value and the increase of potential (*U*), and Pb mainly existed in the forms of organic matter bound and residual in the soil after remediation. Hanay et al. [9] discovered that the type of acid (acetic acid, nitric acid and phosphoric acid) used as washing solution was less effective than the values of pH for removal of Pb from sewage sludge during the ER process. Coupled ER and phytoremediation methods, Aboughalma et al. [10] found that the metal adsorption in plant shoots was lower under DC treatment compared to AC treatment, although there was a higher accumulation of Zn and Cu in the plant roots treated with electrical fields. In addition, the Pb accumulation in the roots and the uptake into the shoots was lower compared to in the soil. Silva et al. [11] investigated ER processes for removing Pb(II) in contaminated soils, and concluded that the significant reduction of the germination in the anodic and cathodic regions for ER by applying DC with $NaNO_3$ and EDTA as cathodic solutions. Yang et al. [12] found that metal (As, Cu, Pb, and Zn) removal was affected by the

initial metal fractionation, metal speciation in the pore solution, and the physical-chemical parameters of the electrolytes (pH and electrolyte composition). Amrate et al. [13] investigated the Pb removal from calcareous soil using EDTA enhanced ER, and noted that the contaminant distribution across the experimental cell indicated the efficient Pb transport toward the anode. Song et al. [14] concluded that EDTA is more effective to enhance *R* of Ni, Pb, and Zn based on ER method, whereas ethylenediaminedisuccinic acid (EDDS) is more effective to increased *R* of Cu. Ng et al. [15] discovered that EDTA test showed the soil alkalisation was achieved, whereas it did not provide significant enhancement on electro migration for Pb and Cr. In the meantime, the power consumption for ER process was decreased by 22.5 %. Kim et al. [16] pointed out that the *R* for Pb and Cd are significantly affect by *U* and current (*I*), purging solutions, pH, permeability and zeta potential. The *R* for Pb and Cd in kaolinite soil during 75-85% and 50-70% in the tailing soil after 4 days treatment. Pedersen et al. [17] found the placement of the anode directly in the soil did not significantly effect on the removal of Al, Mg, Mn, As and Pb in the shooting range soils, whereas moderately influencing the Cu removal. Zhang et al. [18] pointed out that the *R* of the contaminated soil of the anode approaching method only attained 25.93% for Cd and 31.27% for Pb, which was significant higher than that 17.96% and 30.40% obtained by an traditional ER method. Pedersen et al. [19] found that improve the Cu removal could be done by increasing the *I* density, and improve the Pb removal could be done by prolonging the treatment time (*t*) and *I* density. Based on the test results, Kim et al. [20] established a model to describe the Pb(II) transport in the kaolinite under coupled chemical and *U* gradients clay during process of aqueous phase reaction, adsorption, and precipitation, and the validity of the model was confirmed according to comparing the prediction and measured.

The above research results indicate that the ER method has an excellent remediation effect on heavy metal contaminated soil, especially a high application potential for treating Pb contaminated soil. However, the distribution of soil has typical regional characteristics, and existing studies rarely focused on Pb contaminated loess. In this study, ER experiments were conducted on flow-plastic and hard-plastic states of Pb(II) contaminated loess, and the distribution laws of *I*, *U*, pH, Pb(II) concentration (*C*), *R*, and energy consumption (*E*) during ER process were analyzed. The research results have important reference value for guiding the engineering practice.

2. EXPERIMENTAL

2.1 Materials

The loess samples used in the test were collected from soil without heavy metal contamination at a construction site in Xi'an, with a sampling depth of 5-10 m. After the removal of debris, the soil samples were passed through a 2-mm sieve before being dried for later use. Table 1 lists the basic physical properties of the soil samples, Table 2 lists the chemical composition of the loess, and Table 3 lists the main reagents used in the test. The reagents used in the test were of analytical grade.

Table 1. Physical parameters of loess

G_s	w_L (%)	w_P (%)	I_P
2.70	34.2	18.6	15.6

Table 2. Chemical component of loess

Element	Mass percent (%)
SiO_2	64.25
Al_2O_3	11.57
CaO	9.35
MgO	2.99
K_2O	3.15
Fe_2O_3	2.78
Na_2O	2.48
FeO	0.95
TiO_2	0.84
MnO	0.06

Table 3. Main reagent used during the experiment

Reagent	Manufacturer
$Pb(NO_3)_2$	Tianjin Chemical Reagent Co., Ltd
HCl	Tianjin Kemiou Chemical Reagent Co., Ltd
KNO_3	Tianjin Kemiou Chemical Reagent Co., Ltd
$C_6H_8O_7$	Tianjin Kemiou Chemical Reagent Co., Ltd
$C_{10}H_{16}N_2O_8$	Tianjin Kemiou Chemical Reagent Co., Ltd
CH_3COOH	Tianjin Kemiou Chemical Reagent Co., Ltd

2.2 Test equipment

The ER test equipment is shown in Figure 1, and it mainly include a model box, a DC power supply, a *I* and *U* measurement system, an electrolyte circulation system, an overflow collection system, and a data acquisition system. The model box was made of plexiglass, with a size of 310 mm (length)×90 mm (width)×120 mm (height). Among them, the size of the sample chamber was 100 mm×70 mm×100 mm, the size of the electrode chamber was 70 mm×70 mm×100 mm, and the size of the electrode was 70 mm×100 mm. The electrode chamber and the sample chamber were separated by double-layer porous plexiglass plates. During the test, filter paper was placed between the two

plexiglass plates to prevent soil particles from entering the electrode chamber. Small holes were situated at the bottom of the electrode chambers on both sides of the soil chamber for the peristaltic pump to pump the circulating electrolyte into the electrode chamber. Overflow holes were opened on both sides of the electrode chamber, and their positions were flush with the soil after loading to ensure that the upper surface of the soil was not covered by electrolyte during the test. The main instruments and equipment used in the test are shown in Table 4.

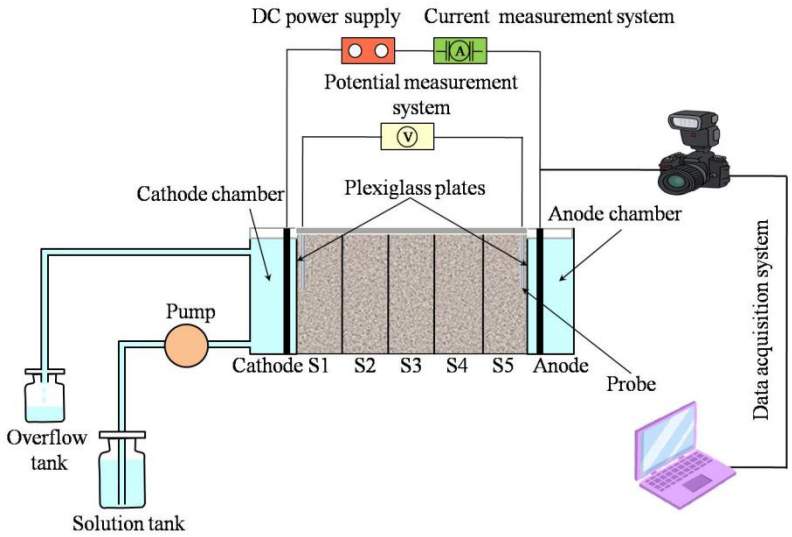

Figure 1. Test equipment

Table 4. Main instrument and equipment

Instrument	Manufacturer
GPS-2303CDC stabilized power	Good Will Instrument Co., Ltd
DHG-9011A drying oven	Shanghai Jinghong Laboratory Instrument Co., Ltd
CT15RT freezing high speed centrifuges	Shanghai Tianmei Biochemical Instrument and Equipment Engineering Co., Ltd
CP214 analytical balance	OHAUS Instrument (Shanghai) Co., Ltd
FIVEEASY PLUS28 pH meter	Mettler Toledo Instrument (Shanghai) Co., Ltd
AA60000 atomic absorption spectrometer	Shanghai Tianmei Biochemical Instrument and Equipment Engineering Co., Ltd
VC86E digital multimeter	Double King Industrial Holdings Co., Ltd
YZ15 peristaltic pump	Baoding Lead Fluid Technology Co., Ltd

2.3 Test scheme

In this test, a total of six groups of Pb(II) contaminated loess samples were subjected to ER tests, as shown in Table 5. During the test, ruthenium-iridium coated titanium mesh was used as the electrode, the *U* was set to 3 V/cm, and 0.1 mol/L KNO_3 was used as the anolyte. The time of each test

was 7 days, and the test was repeated for each set of test settings. To analyze the impact of different consistency states of the contaminated soil, the water content of the contaminated soil in groups T1 to T3 was set to 20% (hard-plastic state), and the sample density was 1.68 g/cm^3. The water content of the contaminated soil in groups T4 to T6 was set to 50% (flow-plastic state), and the sample density was 1.72 g/cm^3.

Table 5. Test scheme

Test No.	Catholyte	Method
T1	0.1 mol/L KNO_3	--
T2	0.1 mol/L KNO_3	Changing electrode at 84 h interval
T3	0.1 mol/L KNO_3+0.15 mol/L citric acid	--
T4	0.1 mol/L KNO_3+0.20 mol/L acetic acid	--
T5	0.1 mol/L KNO_3+0.20 mol/L acetic acid	Stirring soil chamber at 24 h interval
T6	0.1 mol/L KNO_3+0.20 mol/L acetic acid	Pretreatment by 0.2 mol/L acetic acid, and stirring soil chamber at 24 h interval

(1) Preparation of soil samples

To prepare the Pb(II) contaminated soil sample with a concentration of 1000 mg/kg, firstly, 2 kg of dried loess and sufficient distilled water were measured, and 3.1969 g of $Pb(NO_3)_2$ was dissolved in a beaker. Subsequently, the $Pb(NO_3)_2$ solution was added to the dry soil, and the beaker and glass rod were washed with distilled water two to three times. Then, distilled water was added to the soil until the soil was in a flow-plastic state, and the soil sample was stirred with a stirrer for 1 h to allow the Pb(II) to be evenly distributed in the soil. Finally, the soil was dried and crushed. During the crushing process, water was sprayed by a watering can to prevent the generation of toxic dust, and the crushed soil was passed through a 2-mm sieve for later use. After the sample was loaded, the electrolyte was injected into the electrode chamber, followed by 48 h equilibration.

(2) Take samples

After the test, four thin metal sheets were inserted into the soil sample chamber with an interval of 2 cm, and the soil was divided into five equal parts. A spoon was used to dig out the soil, the areas from the cathode to the anode were labeled as S1-S5 sequentially, and the soil was dried for testing.

(3) Measurement of current and potential

The *I* and *U* were measured by a digital multimeter, the *U* on the sample chamber was measured, and the *I* of the entire system was measured. During the test, a timed camera system was used to take the *I* and *U* readings, and then the data were collected.

(4) Measurement of pH

During the pH measurement of the soil sample, 5.0 g of the dried soil after the test was placed in a 50-mL polypropylene centrifuge tube and added with 25 mL of distilled water. After the mixture

was shaken for 2 h to fully mix the soil and water, the sample was placed in a high-speed centrifuge and centrifuged at 5000 r/min for 10 min. The supernatant was collected in a 50-mL centrifuge tube, and a pH probe was inserted into the solution and stirred gently until the reading was stable.

During the pH measurement of the electrolyte, 20 mL of electrolyte was placed in a 50-mL centrifuge tube, the pH probe was inserted into the solution and stirred gently until the reading was stable, and the reading was recorded.

(5) Determination of Pb(II) concentration

In the test, a digestion procedure combining step-by-step extraction and a single extraction method was adopted. After multiple measurements, the extraction rate of the HCl group was between 90% and 95%, while the extraction rate of the EDTA group was between 75% and 80%. Therefore, this experiment used HCl as the extractant for Pb(II) contaminated loess. To prevent the reaction of $CaCO_3$ and acid in the loess from causing the sample to overflow from the centrifuge tube, the HCl was added gradually in the first step, then the tube was covered by a lid and shaken several times. Next, the lid was removed to release the gases until no obvious gas was produced. After a corresponding fold-dilution of the obtained solution, the Pb(II) C was measured with a atomic absorption spectrophotometer.

The Pb(II) removal efficiency was calculated as follows:

$$R = \frac{(m_0 - m_e)}{m_0} \times 100\% \quad (1)$$

where R is the removal efficiency, %; m_0 is the initial total mass of pollutants, mg; and m_e is the total mass of remaining pollutants, mg.

(6) Calculation of energy consumption

The E of ER was calculated as follows:

$$E_c = \frac{1}{M_c} \int UIdt \quad (2)$$

where E_c is the electric consumption for removing a unit mass of pollutants, W·h/mg; M_c is the total amount of pollutants removed, $M_c=m_0-m_e$, mg; U is the potential, V; I is the current, A; and t is the treatment time, h.

3. RESULTS AND DISCUSSION

3.1 Distribution of current during electrokinetic remediation

Current density is related to the counting of mobile ions in the solution of ER process, thereby affecting the ER efficiency [21]. Figure 2 shows the curves of I versus t for Pb(II) contaminated loess during ER. Although a constant U (30 V) was maintained between the two electrodes during the test, the I was characterized by irregular fluctuations. Figure 2(a) shows that for the hard-plastic state, the I of T1 increased (0-10 h) and then decreased (10-20 h) over time, which was similar to the distribution pattern reported in the reference [3].

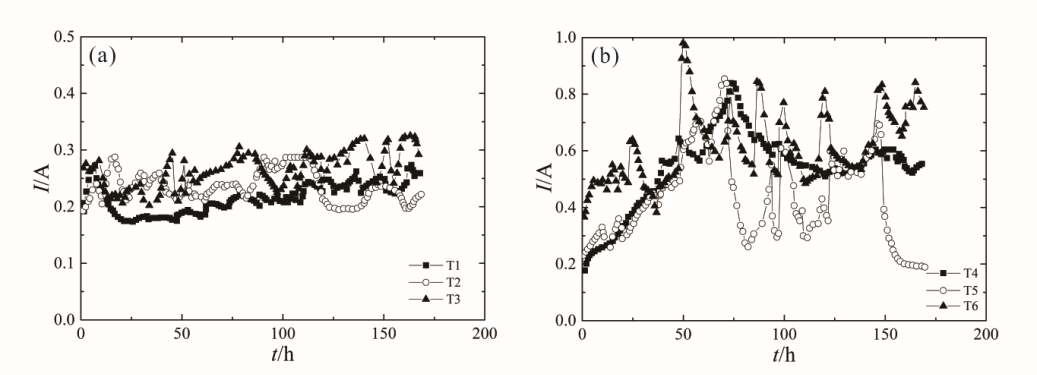

Figure 2. Curves of current versus treatment time during electrokinetic remediation with 30 V potential, 7 d treatment time, and 0.1 mol/L KNO_3 catholyte (a) hard-plastic state (T1-T3) (b) flow-plastic state (T4-T6)

The *I* of T2 increased and then decreased after the electrode was inverted (84 h), and the "focusing effect" can be reduced to an extent by exchanging polarity method [22]. The range of *I* fluctuation of T3 was relatively large, and over time, the *I* decreased after the initial increase, followed by repeated upward and downward fluctuations. The above phenomenon is mainly caused by the generation of much white precipitate in the cathode chamber, which blocks ion migration and causes repeated *I* fluctuations. Figure 2(b) shows that for the flow-plastic state, the average *I* was considerably greater than that of the hard-plastic state. Overall, the *I* first increased and then decreased over time. T4 reached a peak value (0.83 A) at 70 h and then gradually stabilized (at approximately 0.6 A) after 90 h. Comparing the test results of T4 and T3 shows that the *I* of T4 was substantially greater than that of T3. The main reason is that the electrolyte added to the cathode in T3 was citric acid, which reacts with $CaCO_3$ in the loess to produce calcium citrate. Calcium citrate is slightly soluble in water, and it easily blocks the pores in the soil, thereby reducing the permeability of the soil. From the test of T3, the formation of a layer of white precipitate with a thickness of approximately 0.5 cm was observed on the cathode separator, and many holes in the porous separator of the cathode were blocked by the white precipitate, resulting in a decrease in electrical conductivity. In the test of T4, the formation of white precipitates was not observed at the cathode, mainly because calcium acetate is easily soluble in water, so the electrical conductivity of T4 was larger than that of T3.

3.2 Distribution of potential during electrokinetic remediation

Figure 3 shows the curves of *U* versus *t* of Pb(II) contaminated loess during ER. Figure 3(a) shows that for the hard-plastic state, the overall *U* change was highest in T1, followed by T2 and then T3. Among them, the *U* of T1 initially increased, then decreased, and eventually fluctuated, in contrast to the pattern of *U* distribution in the reference [4]. The *U* of T2 increased first and then decreased after the electrode was inverted (84 h), and the *U* of T3 increased first, then decreased, increased again, and then decreased. Figure 3(b) shows that the range of *U* variation in the flow-plastic state was

similar to that of the hard-plastic state. Among them, the *U* of T5 showed periodic fluctuations after 50 h, which was related to the periodic stirring of the soil during the test.

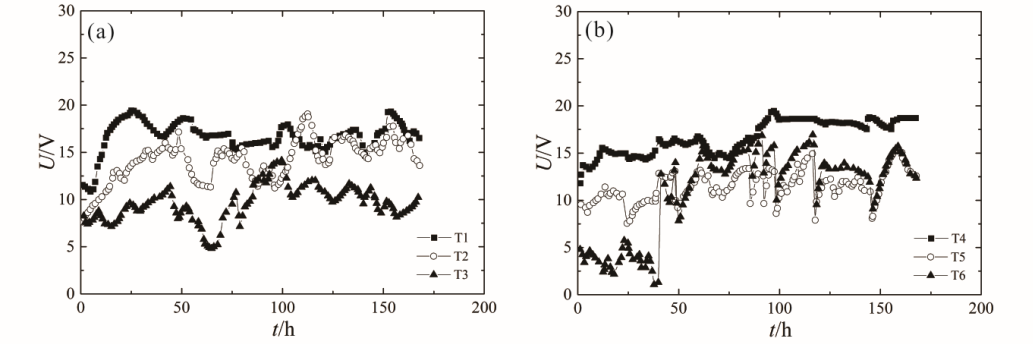

Figure 3. Curves of potential versus treatment time during electrokinetic remediation with 30 V potential, 7 d treatment time, and 0.1 mol/L KNO_3 catholyte (a) hard-plastic state (T1-T3) (b) flow-plastic state (T4-T6)

During the stirring process, more $CaCO_3$ in the soil will be exposed to the acidic environment, and more free ions will be generated after the reaction of $CaCO_3$ and acid, thus facilitating the reaction of Pb(II) with CO_3^{2-} to form $PbCO_3$, which precipitates in the loess. According to the combination of test results between *U* and *I*, the resistances in the soil followed the order T4>T5>T6. It can be concluded that stirring or pre-acidification treatment can reduce the resistance of the soil, thus improving the ER efficiency.

3.3 Distribution of pH in the electrolyte and soil during electrokinetic remediation

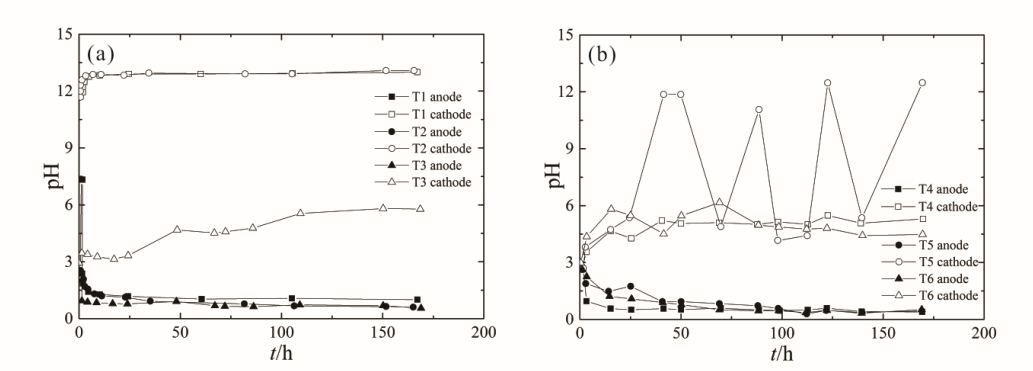

Figure 4. Curves of electrolyte pH versus treatment time during electrokinetic remediation with 30 V potential, 7 d treatment time, and 0.1 mol/L KNO_3 catholyte (a) hard-plastic state (T1-T3) (b) flow-plastic state (T4-T6)

Figure 4 shows the curves of electrolyte pH versus time during the ER. Figure 4(a) shows that for the hard-plastic state, when the catholyte pH was not controlled (T1 and T2), the catholyte pH

reached approximately 13 within 2 h, while the anolyte pH reached approximately 1 within 2 h and remained stable, which consistent with the results of reference [23]. When citric acid was used to control the pH of the cathode (T3), the initial pH of the electrolytes was 2.0, and the pH of the anolyte decreased to approximately 1 within 2 h after the start of the test and remained stable, while the pH of the catholyte gradually stabilized between 5 and 6 at approximately 110 h after the start of the test. By comparison, in the tests in which the pH of the cathode was not controlled, the catholyte pH reached 13 quickly, and the OH^- produced by electrolysis continued to enter the soil, making the environment alkaline. In an alkaline environment, Pb(II) precipitates and becomes less active, which is unfavorable for the removal of Pb(II). Therefore, controlling the catholyte pH is an effective method to improve efficiency of ER. Figure 4(b) shows that, similar to the test results of T3, the catholytes of T4-T6 were always acidic under the control of the pH of the cathode, which may allow the Pb(II) that migrated to the cathode to remain active. T5 followed the same trend as T4 and T6 in the first 24 h, and the catholyte pH increased to approximately 12 after 24 h and then fluctuated between 5 and 12. Due to the flow-plastic soil in T5 was stirred every 24 h, the $CaCO_3$ in the loess reacted with acetic acid to produce numerous bubbles, which consumed a large amount of acetic acid. The buffering effect of the circulating catholyte weakened at a constant pumping rate, thereby the catholyte pH changed periodically. The method of stirring at intervals of 24 h was also used in T6, whereas the loess in T6 had been acidified before the test, resulting in limited $CaCO_3$ content, thereby the periodic fluctuation of the catholyte pH in T5 did not occur in T6.

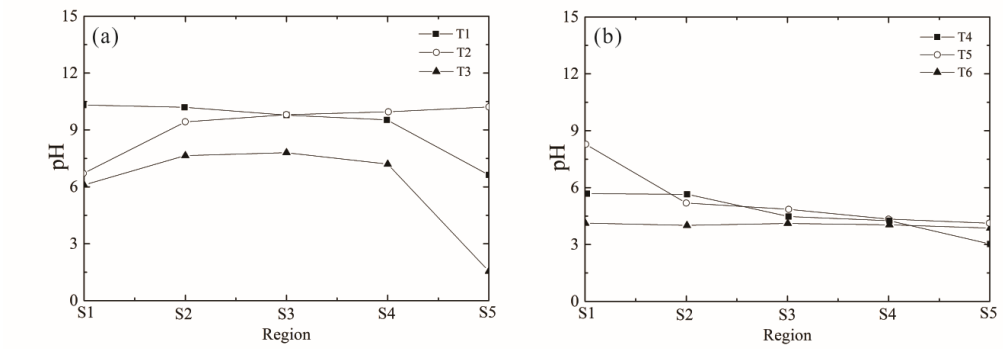

Figure 5. Curves of soil pH versus region after electrokinetic remediation with 30 V potential, 7 d treatment time, and 0.1 mol/L KNO_3 catholyte (a) hard-plastic state (T1-T3) (b) flow-plastic state (T4-T6)

Figure 5 shows the curves of soil pH versus region during ER. Under ER process, the whole region was divided into an acidic area and an alkaline area when H^+ and OH^- met in the process of moving [21]. Figure 5(a) shows that the soil pH in T1 increased in most regions while only decreasing slightly in the region near the anode compared with that of the original soil. The migration speed of H^+ was greater than that of OH^-, so the acid-base boundary zone was usually close to the cathode (near S2) in the ER test, while the acid-base boundary zone in T1 appeared between S4 and S5. The main reason for this behavior is that the $CaCO_3$ content of the loess used in the experiment was 11.25%, and similar phenomena usually occur in the ER of the soil with high carbonate content. Since the electrode

was inverted in T2 at 84 h, the pattern of pH distribution in the soil after the test was opposite to that of T1. In T3, the pH of the soil in S5 dropped to approximately 1, while the pH of the soil in S2, S3, and S4 was basically the same as or slightly higher than that of the original soil. Citric acid was used in the cathode of T3 to control the pH of the catholyte, which caused the environment of the cathode to be acidic during the test. At the end of the test, the catholyte pH was between 5 and 6. The pH of the soil in S1 was approximately 6, indicating that when the pH of the catholyte was controlled, the pH of the soil in S2, S3, and S4 did not change greatly. Figure 5(b) shows that, consistent with the pattern of distribution in the references [1, 3, 18], the pH of the soil was higher near the cathode region and lower near the anode region due to the alkaline pH registered in the catholyte [24, 25]. After the tests in T4 and T6, the soil pH was acidic, while T5 was weakly alkaline because of the decrease in the buffer capacity of the circulating catholyte. The soil in T6 was pretreated with acid, thereby it had the lowest overall pH and the smallest change in pH.

3.4 Distribution of concentration and removal efficiency after electrokinetic remediation

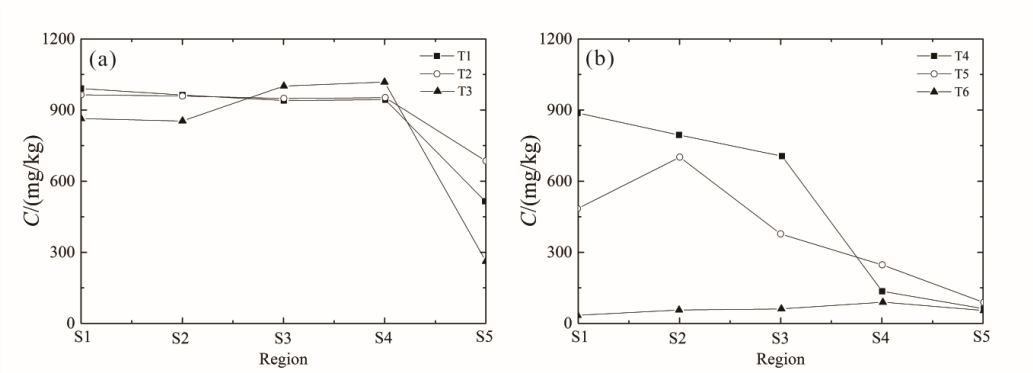

Figure 6. Curves of Pb(II) concentration versus region after electrokinetic remediation with 30 V potential, 7 d treatment time, and 0.1 mol/L KNO_3 catholyte (a) hard-plastic state (T1-T3) (b) flow-plastic state (T4-T6)

Figure 6 shows the curves of Pb(II) *C* versus region during the ER. Figure 6(a) shows that in the tests of T1, T2, and T3, the Pb(II) content in S5 was relatively low, and the changes in Pb(II) content in other regions were small. The removal of Pb(II) in T1 and T2 was mainly concentrated in S5, and the residual amount of Pb(II) in S5 in T1 was less than that in T2. A possible reason for the above phenomenon is that the time of S5 in T1 at the anode is longer than that of T2 (electrode inversion at 84 h). Meanwhile, Pb(II) content increased in S1 in T1 but not in T2. A possible reason is that after the electrode inversion, S1 in T2 contacted the acidic electrolyte, which helped remove Pb(II). In T3, the Pb(II) contents in S1, S2, and S5 decreased to varying degrees, while Pb(II) enrichment occurred in S3 and S4. Figure 6(b) shows that the Pb(II) *C* in the soil was lower near the anode and higher near the cathode, which was consistent with the pattern of distribution in the references [10, 18], indicated that the Pb(II) removal efficiency was better near the anode side [24]. Overall, the Pb(II) *C* in the soil of T4, T5 and T6 after the tests were significantly lower than those of

T1, T2 and T3, indicating that the method of adding catholyte and stirring at a interval time is conducive to removing Pb(II) from soil.

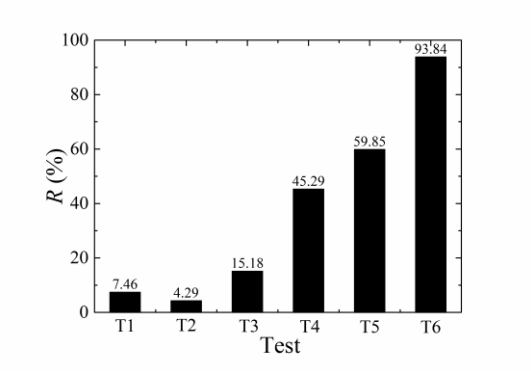

Figure 7. Histogram of Pb(II) removal efficiency after electrokinetic remediation with 30 V potential, 7 d treatment time, and 0.1 mol/L KNO_3 catholyte

Figure 7 shows the histogram of Pb(II) *R* during the ER. The figure shows that the Pb(II) *R* at the end of the six groups of experiments were in descending order, T6>T5>T4>T3>T1>T2. As the test results of reference [3], citric acid and acetic acid could significantly enhanced the removal efficiency of Pb(II). Among them, the Pb(II) *R* of T6 was the highest, reaching 93.84%, while the Pb(II) *R* of T2 was the smallest, only 4.29%. It can be seen that by adding catholyte, acidizing the soil in advance, stirring the soil at a interval time, and increasing the *U* [6], the Pb(II) *R* can be substantially increased, and the ER efficiency of contaminated soil can be improved.

3.5 Analysis of energy consumption during electrokinetic remediation

Table 6. Removal efficiency and energy consumption

Test No.	Removal efficiency (%)	Energy consumption (kW·h)	E_c (W·h/mg)
T1	7.46	1.08	21.03
T2	4.29	1.19	40.55
T3	15.18	1.32	12.70
T4	45.29	2.69	10.10
T5	59.85	2.18	6.20
T6	93.84	3.09	5.60

High *E* is one of the major setbacks of ER method, and the *E* is a direct function of the *U* [26]. In general, better remediation effects usually correspond to higher *E*, thereby a balance among the *R*, *E* as well as *t* needs to be considered for real applications [25]. Table 6 summarizes the Pb(II) *R* and *E* in six group of experiments. The table shows that when the electrokinetic enhancement method was not

used, the results were consistent with the pattern of change in the reference [8], in which the Pb(II) *R* was low, the *E* was low, and the average *E* was high. When the electrokinetic enhancement method was used to increase the Pb(II) *R* of the contaminated soil, the *E* increased correspondingly, but the average *E* decreased, indicating that the efficiency of ER was improved. Therefore, when the ER method is used to treat Pb(II) contaminated loess in engineering practice, corresponding electrokinetic enhancement methods (adding catholyte, acidizing treatment, stirring, etc.) should be adopted to improve the ER efficiency of contaminated soil.

4. CONCLUSIONS

(1) The *I* and *U* of different tests exhibited irregular trends over time. The range of *I* change in the flow-plastic state was considerably larger than that of the hard-plastic state, while the ranges of *U* change in the two were slightly different. According to the *I* and *U* test results, it can be concluded that stirring or pre-acidizing treatment can reduce the electrical resistance of the soil, thereby improving the ER efficiency.

(2) When the electrolyte was not added to the cathode, the catholyte pH reached 13 quickly, and the resultant alkaline environment resulted in precipitation and decreased activity. When the electrolyte was added to the cathode, the Pb(II) that migrated to the cathode maintained high activity. As a result, the pH in the soil gradually decreased from the cathode to the anode after the test was completed, and the pH of the soil in different regions was between 3 and 6.

(3) The Pb(II) *R* reached 93.84% for T6, whereas was only 4.29% for T2. Adding electrolyte to the cathode, pre-acidizing the soil, and stirring at a interval time can considerably increase the Pb(II) *R* and improve the efficiency of ER of contaminated soil.

(4) The application of the electrokinetic enhancement method resulted in a larger Pb(II) *R*, higher *E*, and lower average *E*, indicating an improvement in the efficiency of ER.

(5) When citric acid was used as the electrolyte, the soil pores were blocked, and the overall *R* was only 15.18%; when acetic acid was used as the electrolyte, the Pb(II) *R* was increased to over 45.29%, indicating that acetic acid is more suitable for enhancing the effect of ER.

ACKNOWLEDGEMENTS
This work was supported by the Natural Science Basic Research Program of Shaanxi Province (2021JM-535), and Special Fund for Scientific Research by Xijing University (XJ18T01).

CONFLICT OF INTEREST
On behalf of all authors, the corresponding author states that there is no conflict of interest.

DATA AVAILABILITY
The data used to support the findings of this study are available from the corresponding author upon request.

References

1. H. K. Hansen, L. M. Ottosen, B. K. Kliem and A. Villumsen. *J. Chem. Tech. Biotechnol*., 70 (1997) 67.
2. H. Beyrami. *Chin. J. Chem. Eng*., 2020, Doi: 10.1016/j.cjche.2020.09.011.
3. G. Asadollahfardi, M. S. Sarmadi, M. Rezaee, A. Khodadadi-Darban, M. Yazdani, and J. M. Paz-Garcia. *J. Environ. Manage*., 279 (2021) 111728.
4. W. Zulfiqar, M. A. Iqbal and M. K. Butt. *Chemosphere*, 169 (2017) 257.
5. H. Han, J. Zhai, A. W. Wang, J. Li, C. D. Xu and Y. S. Wan. *Agric. Biotechnol*., 9 (2020) 73.
6. T. Huang, L. L. Zhou, L. F. Liu and M. Xia. *Waste Manage*., 75 (2018) 226.
7. I. Tahmasbian and A. A. S. Sinegani. *Environ Monit Assess*., 185 (2013) 8847.
8. Z. C. Zhang, W. T. Ren, J. Zhang and F. Zhu. *Environ. Technol*., 42 (2021) 884.
9. O. Hanay, H. Hasar, N. N. Kocer and O. Ozdemir. *Environ. Technol*., 30 (2009) 1177.
10. H. Aboughalma, R. Bi and M. Schlaak. *J. Environ. Sci. Health, Part A*., 43 (2008) 926.
11. K. N. O. silva, S. S. M. Paiva, F. L. Souza, D. R. Silva, C. A. Martinez-Huitle and E. V. Santos. *J. Electroanal. Chem*., 816 (2018) 171.
12. J. S. Yang, M. J. Kwon, J. Choi, K. Baek and E. J. O'Loughlin. *Chemosphere*, 117 (2014) 79.
13. S. Amrate, D. E. Akretche, C. Innocent and P. Seta. *Sci. Total Environ*., 349 (2005) 56.
14. Y. Song, M. T. Ammami, A. Benamar, S. Mezazigh and H. Q. Wang. *Environ SciPollut Res*., 23 (2016) 10577.
15. Y. S. Ng, B. S. Gupta and M. A. Hashim. *Environ SciPollut Res*., 23 (2016) 546.
16. S. O. Kim, S. H. Moon and K. W. Kim. *Water, Air, Soil Pollut*., 125 (2001) 259.
17. K. B. Pedersen, P. E. Jensen, L. M. Ottosen and J. Barlindhaug. *Eng. Geol*., 238 (2018) 52.
18. P. Zhang, C. J. Jin, Z. F. Sun, G. H. Huang and Z. L. She. *Water, Air, Soil Pollut*., 227 (2016) 217.
19. K. B. Pedersen, P. E. Jensen, L. M. Ottosen and J. Barlindhaug. *J. Hazard. Mater*., 368 (2019) 869.
20. S. O. Kim, J. J. Kim, K. W. Kim and S. T. Yun. *Sep. Sci. Technol*., 39 (2004) 1927.
21. Y. J. Zhang, G. H. Chu, P. Dong, J. Xiao, Q. Meng, M. Baumgartel, B. Xu and T. Hao. *J. Soils Sediments*, 18 (2018) 1915.
22. Z. P. Cai, J. van Doren, Z. Q. Fang and W. S. Li. *Trans. Nonferrous Met. Soc. China*, 25 (2015) 3088.
23. A. Missaoui, I. Said, Z. Lafhaj and E. Hamdi. *Mar. Pollut. Bull*., 113 (2016) 44.
24. O. Karaca, C. Cameselle and K. R. Reddy. *Environ. Earth. Sci*., 76 (2017) 408.
25. C. Li, H. J. Hou, J. K. Yang, S. Liang, Y. F. Shi, R. N. Guan, Y. Hu, X. Wu, J. P. Hu and L. L. Wang. *Clean: Soil, Air, Water*, 47 (2019) 1800337.
26. A. K. Usman, N. D. Mu'azu, S. Lukman, M. H. Essa, A. A. Bukhari and M. H. Al-Malack. *Soil Sediment Contam*., 29 (2020) 465.